Hindawi Publishing Corporation
Advances in Meteorology
Volume 2016, Article ID 8364134, 13 pages
http://dx.doi.org/10.1155/2016/8364134

Research Article

Severe Weather Caused by Heat Island and Sea Breeze Effects in the Metropolitan Area of São Paulo, Brazil

Felipe Vemado and Augusto José Pereira Filho

Departamento de Ciências Atmosféricas, Instituto de Astronomia, Geofísica e Ciências Atmosféricas, Universidade de São Paulo, 05508–090 São Paulo, SP, Brazil

Correspondence should be addressed to Felipe Vemado; vemado@model.iag.usp.br

Received 18 June 2015; Revised 21 August 2015; Accepted 3 September 2015

Academic Editor: Shahaboddin Shamshirband

The Metropolitan Area of São Paulo (MASP) is one of the most populated regions of the planet with one of the largest impervious regions as well. This research work aims to characterize MASP heat island (HI) effect and its interaction with the local sea breeze (SB) inflow in rainfall amounts and deep convection. The combined SB-HI produces direct circulation over the MASP and produces severe weather and socioeconomic impacts. All SB-HI episodes between 2005 and 2008 are identified and analyzed with surface and upper air measurements, weather radar, and satellite data. The current work indicates that intense SB-HI episodes are related to air and dew point temperatures above 30°C and 20°C, respectively, right after the passage of the SB front over MASP. Results indicate that the precipitation related to SB-HI episodes is up to 600 mm or about four times higher than that in rural or less urbanized areas in its surroundings. Measurements indicate that 74% of SB-HI episodes are related to NW winds in earlier afternoon hours. Moving cold fronts in southern Brazil tend to intensify the SB-HI circulation in MASP. A conceptual model of these patterns is presented in this paper.

1. Introduction

The Metropolitan Area of São Paulo has 39 municipalities with São Paulo city being the largest one with an area of 8051 km^2 with a 20 million population according to Brazilian Geography Institute, 2010. Frequently, severe weather systems cause major socioeconomic impacts in the São Paulo megacity such as the ones related to cold fronts, sea breeze circulation, mesoscale convective systems, and isolated convection [1–3] with heavy rainfall, wind gusts, hailstones, and lightning. SB circulation reaches MASP more than half of the days throughout the year. Oliveira and Dias [4] analyzed several instances of sea breeze (SB) and indicated wind veering from NE to SE, backing from NW to SE, and intensification of the SE wind. Pereira Filho et al. [5] studied the SB and HI effects on rainfall accumulation in the Metropolitan Area of São Paulo (MASP) and found that weak synoptic conditions, air temperature, and dew point above 30°C, respectively, in the afternoon hours tended to result in heavy precipitation. Oliveira and Dias [4] reported many instances of summer convection in the MASP preceded by changes in wind direction from NW to SE associated with temperature drop and dew point temperature increase. The SB intensifies as it moves across Serra do Mar ridge and injects Atlantic Ocean moisture in the MASP. The SB intensity and inland displacement are modulated by the HI effect in the MASP [6, 7], and the distance propagated over landmass [8], topography, and atmospheric stability [9]. The differential heating in the Serra do Mar ridge induces vertical motion along its steep scarp (Figure 1) and intensifies the SB circulation along the mountain range [10, 11]. Pereira Filho et al. [1] analyzed 18 episodes of floods in MASP associated with SB (Figure 2). Vertical mixing of relative warmer and drier urban boundary layer air with relatively cooler and moister SB air at its frontal region turns the air unstable and updrafts develop to deep convection driven by latent heat release. The effect of large urban areas on rainfall is an issue of several research works. Shepherd et al. [12] used the Tropical Rainfall Measurement Mission (TRMM) satellite to confirm the increase of rainfall downwind urban areas

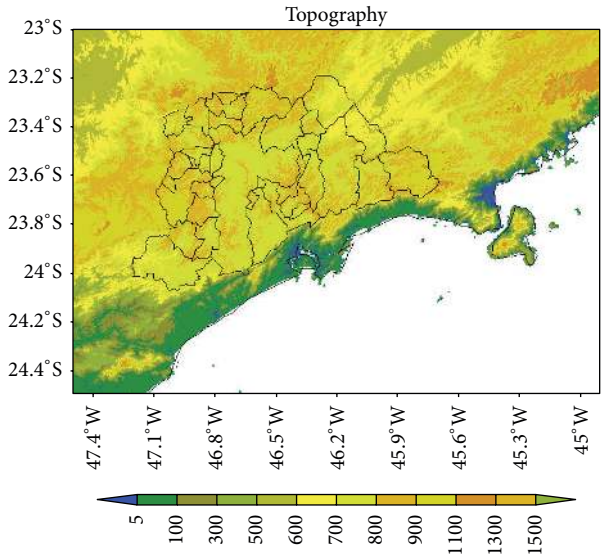

Figure 1: Topography of Eastern São Paulo State. Contours, geographic coordinates, and political boundaries are indicated. Color bar indicates altitudes (m).

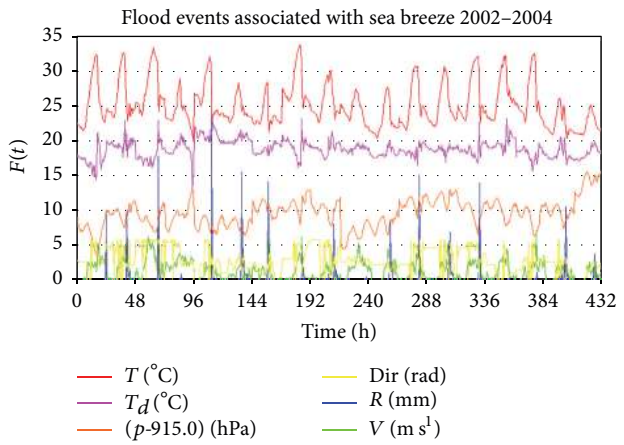

Figure 2: Temporal evolution of air temperature (red), dew point (pink), atmospheric pressure (orange), rainfall accumulated (blue), wind direction (yellow), and wind intensity (green) of 18 floods events. Font: Pereira Filho et al. [1].

of USA. Accumulated and rainfall rate increases with the increase of the city area. Kusaka et al. [13] showed that urbanization caused an increase in precipitation in Tokyo metropolitan area and less precipitation in inland areas.

The SB circulation in Eastern São Paulo State is so regular that it can be clearly seen in the numerical modeling climatology of hourly winds between 2005 and 2007 as an inertial circulation (Figure 3). Surface winds back NW to SE between 1500 UTC and 1600 UTC over MASP similar to those observed by Oliveira and Dias [4].

This work analyzes all SB events between 2005 and 2008 associated with thunderstorms in MASP as well as synoptic conditions that enhance local circulation and intensity of thunderstorms. SB and synoptic scale timing for maximizing deep convection efficiency is also investigated in the present work. Many studies have characterized the effect of urban areas in precipitation and its spatial distribution but less emphasize on temporal and spatial phase looking at different systems scales. The results of this research can be a useful nowcasting rule for MASP and other similar metropolitan areas of the planet.

Urban Heat Island. The temperature gradient between urban areas and their surrounding areas is called urban heat island (UHI) [14]. The average annual temperature in the inner city is higher than in the surroundings. In dry winter days, the temperature gradient can reach 10°C or more in the late afternoon and early evening [15, 16]. The temperature difference between urban and rural New York City is 5°C during nighttime in summer [17]. The UHI is characterized by anthropic sources of heat within urban areas that absorbs short wave irradiation and converts it into sensible heat [18]. Under clear sky conditions and during the night, the temperature is more dependent on microscale urban features [19].

The UHI is a microclimate change of anthropic nature, changing rural surfaces to urban ones altering energy fluxes of latent heat (less) and sensible heat (more). The irradiance is used for evapotranspiration in a rural area, but, in an urban area, it is stored up and increases the sensible heat flux to the atmospheric boundary layer [14, 20]. A thermal low forms and induces convergence and vertical mixing of relatively warmer and drier air near surface with cooler and drier air aloft, so the boundary layer becomes deeper and even drier as surface air temperature increases and dew point decreases until the inflow of SB front. So, UHI environments are in general warmer and drier in relation to rural ones [21].

The MASP topography is complex and varies from 650 m to 1200 m. It is 50 km from the coast of São Paulo State. The SB circulation in MASP is intensified by the Serra do Mar scarps resulting in higher precipitation over it. Since MASP is at tropical latitudes, differential heating tends to induce more intense and persistent direct circulations [22]. The MASP UHI becomes even more intense under weak synoptic conditions [23] and amplifies rural-urban temperature gradients resulting in stronger and deeper thermal circulation between morning and midafternoon when the advection of moisture by the SB increases moist static instability and deep convection develops with subsequent heavy rainfall [1, 2]. Moreover, Han et al. [24] showed that higher aerosol concentration in urban areas results in increased concentration of smaller cloud drops and higher condensational heating that yields stronger updrafts, larger liquid water content, enhanced higher level riming and melting, and, consequently, enhancement of precipitation downwind of the urban area.

Freitas et al. [25] suggested that UHI accelerates the SB front thus yielding longer and intense updrafts. Farias et al. [26] observed higher frequency of negative cloud-to-ground (CG) lightning flashes and lower for positive CG ones over MASP. Their results are similar to other megacities where air pollution and UHI are suggested as main factors [26].

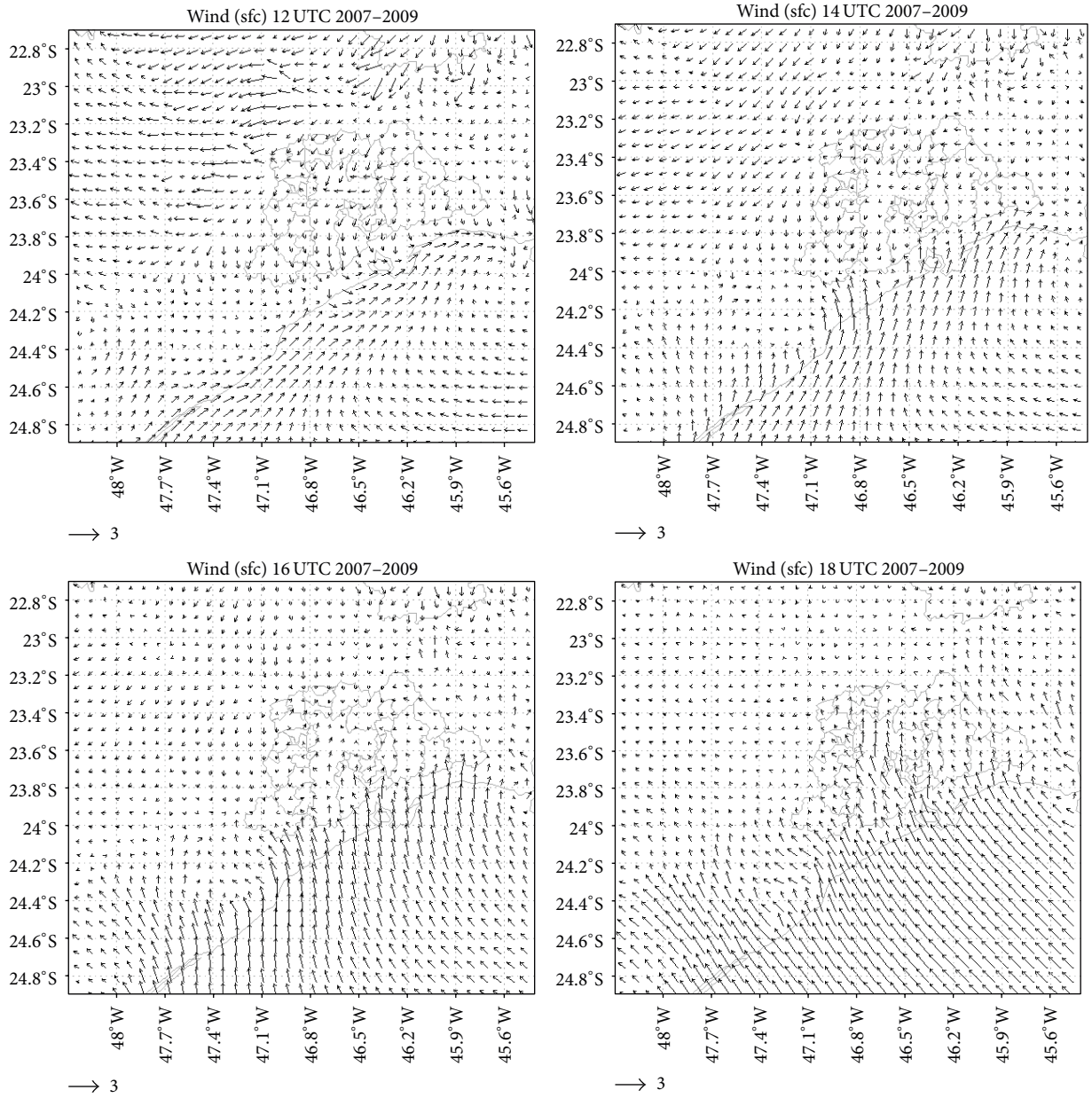

Figure 3: Hourly mean wind ($m\,s^{-1}$) climatology between January 2007 and December 2009 obtained with ARPS simulations. Contours, geographic coordinates, and political boundaries are indicated.

Storms. Storms develop in response to the convective available potential energy (CAPE) in the atmosphere. The storms have been linked to radiative, thermodynamic, and dynamic processes that regularly produce atmospheric instability. These physical processes trigger new dynamic and thermodynamic conditions in a well-defined cycle of events [27]. Convection ceases when CAPE is dissipated or when heat and moist fluxes are interrupted. Convective cells are produced at the local scale under such thermodynamics conditions and influenced by synoptic scale dynamics [28]. Convective forecasting depends on complex thermodynamic, dynamic, and microphysical processes at cloud scale. Thunderstorms develop in a matter of minutes where near-the-surface warm and most air is underlying cold and dry air aloft in association with a lifting mechanism [29]. Atmospheric model performance is limited by unknown triggering mechanisms of convection [30].

Figure 4 shows convective events associated with SB. Vicente et al. [31] indicate that 36% of storms in East São Paulo State between 1990 and 1995 occurred in the afternoon hours. In general, model circulation and precipitation have high and low performance, respectively [32]. Thunderstorms simulated with the Advanced Regional Prediction System (ARPS) [33–36] in MASP indicate that even little changes in boundary and initial conditions can drastically displace the convective cells. However, the ARPS system is able to simulate

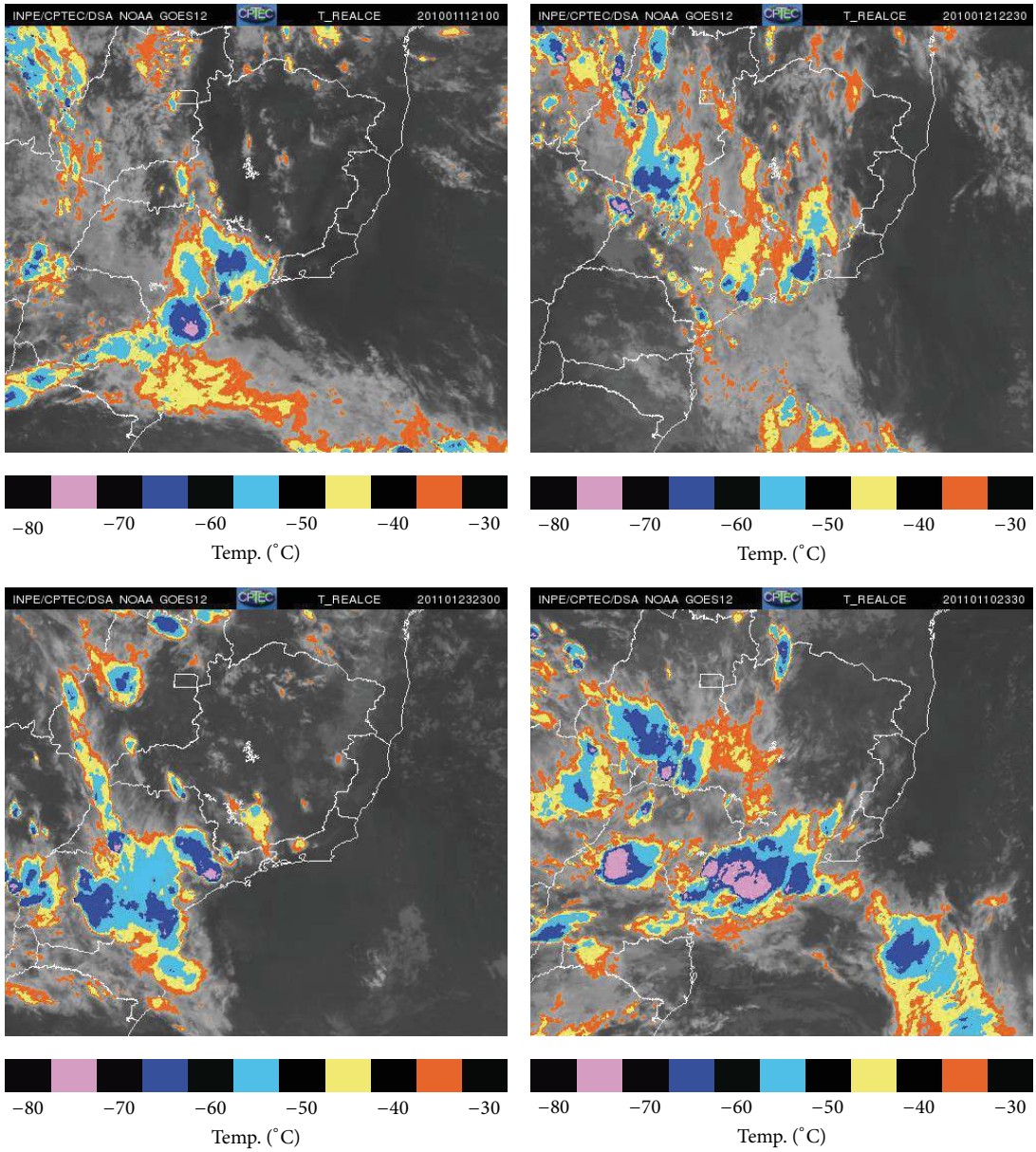

Figure 4: GOES-12 enhanced IR images of cloudiness associated with sea breeze related deep convection events. Contours, geographic coordinates, and political boundaries are indicated. Colors indicated the brightness temperatures. Source: INPE.

the strength of convective cells as well as the interaction between the SB and gust fronts [37, 38] where horizontal vorticity resulting from the SB front and thunderstorm gust fronts result in stronger upward motion [39].

2. Materials and Methods

A total of 125 SB events related to heavy rainfall were selected in three and half years of observations. GOES-8 and GOES-12 Satellites infrared images with 4-km resolution have been used in association with weather station measurements, upper air soundings, the São Paulo weather radar (SPWR), rainfall rate estimates at 3-km altitude, polarimetric variables of the mobile X-POL weather [40], the Global Forecast System (GFS) of National Centers for Environmental Prediction (NCEP), and ARPS. These measurements are briefly described below.

2.1. The São Paulo Weather Radar. The São Paulo S-band weather radar is located at Ponte Nova City near a Serra do Mar ridge at 916 m altitude. It has been operational since 1988. Volume scans are obtained every 5 minutes to estimate rainfall rates [41] at a constant altitude with 2-km × 2-km horizontal resolution. Figure 5 shows an instance of thunderstorms caused by the SB within the surveillance area of the SPWR. Episodes with rainfall rates above 30 mm h^{-1} that lasted for more than 10 minutes related to SB were

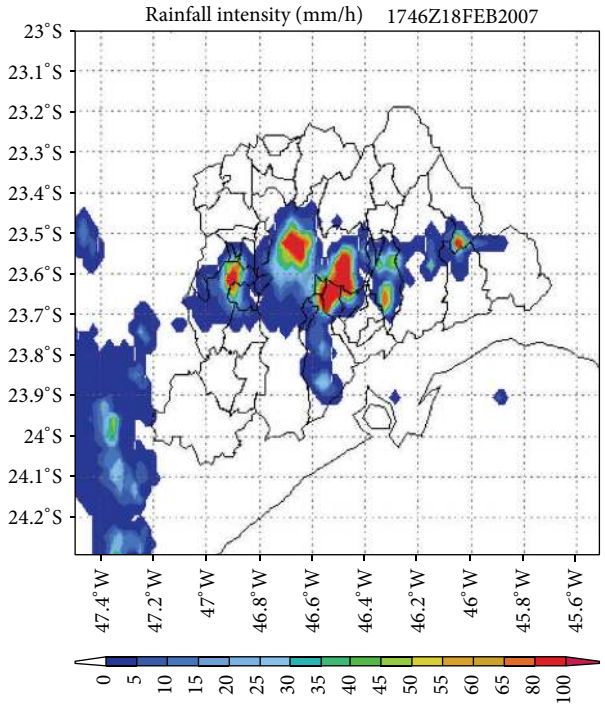

Figure 5: SPRW rainfall rate CAPPI showing thunderstorms at 1746 UTC on February 18, 2007. Color bar indicates rainfall rates ($\mathrm{mm\,hr^{-1}}$).

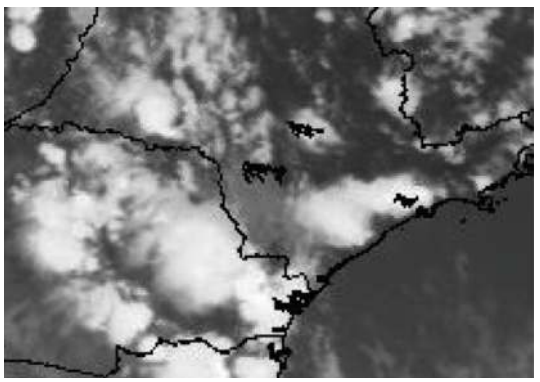

Figure 6: GOES-12 IR image over Eastern São Paulo State at 1800 UTC on January 11, 2010.

selected. Figure 6 shows the respective GOES-12 IR image of the SB episode.

2.2. Satellite GOES-12. GOES-12 IR images provided by CPTEC-INPE were analyzed at 30-minute time intervals. Cloud brightness temperatures below −30°C were enhanced. Figure 4 shows the inset of storms developed by the SB and the UHI circulation.

2.3. Surface Measurement. Temperature (°C), relative humidity (%), air pressure (hPa), wind speed ($\mathrm{m\,s^{-1}}$) and direction (°), precipitation (mm), and cloud cover fraction are regularly measured at Congonhas and Campo de Marte Airports and by the IAG-USP weather station. The datasets were used to select SB episodes between January 2005 and April 2008, using the identification method developed by Oliveira and Dias [4]. These events were identified by changes in wind direction and intensity, air temperature decrease, and dew point temperature increase [4] for days with convective activity in the MASP. Figure 5 shows the estimated rainfall rate field by the SPWR at 1746 UTC February 18, 2007, associated with NW winds that backed to SE after 1500 UTC when the SB front moved into MASP (not shown). Constant SSE winds after the SB front passage were used to select the episodes. Satellite images were also used to verify cloudiness and its depth along the coast of São Paulo State.

2.4. MXPOL Weather Radar. The mobile weather radar X-band Doppler termed MXPOL is a multifunctional system that provides polarimetric data with high spatial resolution [40]. It measures raw and adjusted reflectivity (Z), radial velocity (V_r), spectral width (W), differential reflectivity (Z_{DR}), propagation differential phase (φ_{DP}), specific differential phase (K_{DP}), and correlation coefficient lag zero of the signal co-pol and cross-pol H V ($\rho_{0\mathrm{HV}}$). Its software produces constant elevation (PPI) and altitude (CAPPI) maps, vertical cross-sections (RH), and echo tops (ECHOTOP) of the above variables as well as fields of rainfall accumulation, vertically integrated liquid water (VIL), and others. MXPOL was positioned West of the MASP in Barueri City (Figure 7) at 23° 29′ 59.6″S and 46° 54′ 18.6″W [40]. PPI products at elevations 0.6° and 1.2° were used to identify moving boundaries detected by targets such as shaft, insects, and small cumulus droplets forming in the SB front. Figure 7 shows an episode of SB in late afternoon on January 11, 2010, that produced deep thunderstorms with reflectivity above 55 dBZ (hail).

2.5. Soundings. Radiosounding measurements made at Campo de Marte Airport at 0000 UTC and 1200 UTC were used. The variables are air temperature (°C), dew point (°C), wind speed ($\mathrm{m\,s^{-1}}$) and direction (°), air pressure (hPa), geopotential height (m), water vapour mixing ratio ($\mathrm{g\,kg^{-1}}$), potential temperature (K), virtual potential temperature (K) and equivalent potential temperature (K), convective available potential energy (CAPE) ($\mathrm{J\,kg^{-1}}$), convective inhibition (CINI) ($\mathrm{J\,kg^{-1}}$), and precipitable water (mm). The CAPE (1) and IL index (2) obtained with the soundings were compared to the ones simulated with ARPS system (Section 2.6):

$$\mathrm{CAPE} = g \int_{\mathrm{NCL}}^{\mathrm{NE}} \left(\frac{\theta_{ep(\mathrm{NCL})} - \theta_{esa}}{\theta_{esa}} \right) dZ, \tag{1}$$

where NCL is lifting condensation level (m); NE is equilibrium level (m); θ_{ep} is equivalent potential temperature of an air parcel (K); and θ_{esa} is saturated equivalent environment potential temperature (K);

$$\mathrm{IL} = T_{500} - T'_{500}, \tag{2}$$

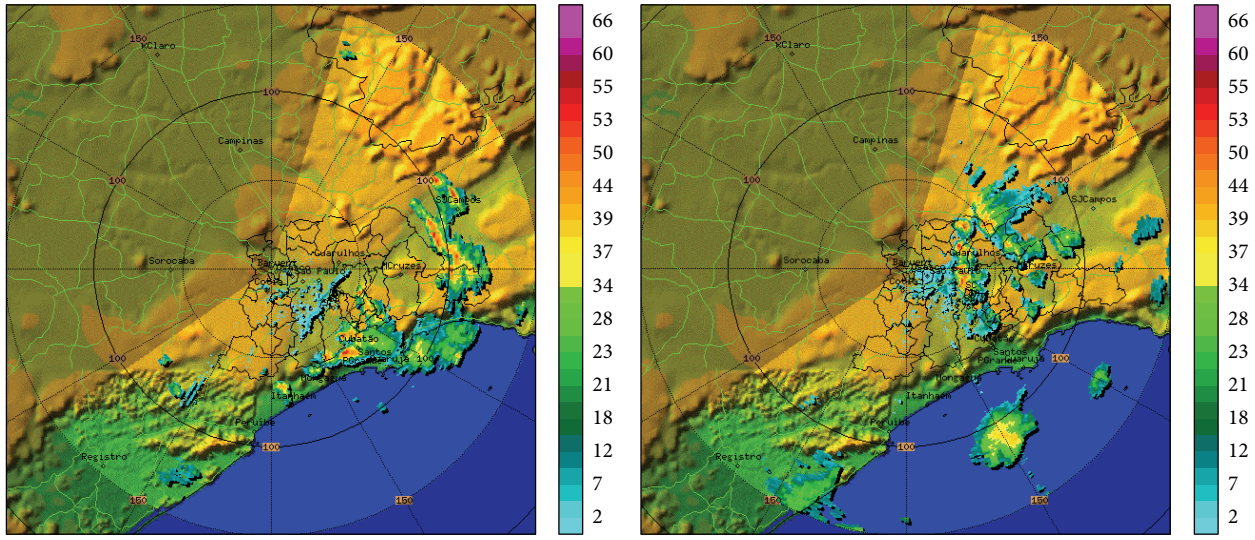

Figure 7: MXPOL PPI of reflectivities (dBZ) at 1800 UTC (a) and 2030 UTC (b) on January 11, 2010. Colors indicate reflectivities (dBZ). Contours, geographic boundaries, radial and azimuthal distances, and political boundaries are indicated.

where T_{500} is air temperature (°C) at 500 hPa and T'_{500} is air temperature (°C) by lifting an air parcel with the mean mixing ratio from 500 hPa.

2.6. The ARPS System. The ARPS system was described by Xue et al. [35, 42]. It runs twice daily since 2005 at the computing facility of Laboratório de Hidrometeorologia (LABHIDRO) at IAG-USP. The domain has two nested grids at 12 km and 2 km resolution. The latter is centered in the MASP region but the former is used in the present work. The boundary and initial conditions were provided by GFS model outputs in the domain shown in Figure 10.

2.7. Global Forecast System (GFS). GFS is a spectral weather forecast model with 64 vertical levels running four times a day by the National Centers for Environmental Prediction (NCEP). It covers the whole globe at a 28-km horizontal resolution. GFS results at 1° resolution were input as boundary and initial conditions to ARPS runs at 12-km spatial resolution. The GFS predicts weather up to 16 days in advance. Its complete documentation can be found at http://www.emc.ncep.noaa.gov/GFS.

3. Results

All SB and UHI heavy rainfall episodes measured with the SPWR were analyzed between 2005 and 2008. The respective synoptic features were obtained with the GFS and the local circulation and instability indexes with the ARPS simulations at 12-km grid resolution.

3.1. Characteristics of SB Episodes. 125 SB episodes were selected with deep thunderstorms in MASP. It was obtained with weather stations that episodes of surface wind veering from NW to SE made up 74% of all of them, 11% from NE to SE, and 15% due to intensification of SE winds during the day. The frequency of storms due to NW winds days agrees with that obtained by Rodriguez et al. [43]. The average dew point temperatures before and after the SB front inflow at IAG's weather station were 17.9°C and 20.7°C, respectively. Similarly, average air temperatures before and after the SB front inflow were 28.6°C and 24.9°C, respectively. At Campo de Marte Airport average air temperatures were 29.7°C and 25.8°C. Noteworthily, the estimates were obtained with data one hour before and one hour after the SB front passage at both weather station locations.

The average SB front speed between both weather stations was 9 m s^{-1}. There have been just four episodes where the SB front did not reach Campo de Marte Airport. Winds were from N to W between 2 and 3 m s^{-1}. The maximum air temperature was less than 27°C and temperature gradients between MASP and Serra do Mar scarp seemed to be considerably lower, consequently the SB dissipated before moving across MASP.

Episodes with dew point temperature less than 15°C before the SB front incoming yielded weak ordinary convective cells and friction quickly dissipates the SB front. However, higher dew point temperatures yielded frequent deeper and stronger convective cells. Downdrafts and gusts near the rear flank induced its faster displacement by cooling downdrafts resulting from higher temperature gradients near the surface about the SB front. Under clear air condition and low dew point, the UHI intensifies [19] and so to produce convective cells over MASP the SB circulation needs to be deeper and stronger.

Most episodes of heavy precipitation associated with SB occur between October and April. Table 1 shows our results about the mean time of SB front passage at IAG's weather station estimated with Oliveira and Dias [4] method.

Table 1: Mean time of SB incoming in each weather station. LT indicates local time.

Year	Campo de Marte airport (SBMT)	Congonhas airport (SBSP)	IAG-USP (Cientec)
2005	1936 UTC (17:36 LT)	1827 UTC (16:27 LT)	1817 UTC (16:17 LT)
2006	1912 UTC (17:12 LT)	1815 UTC (16:15 LT)	1809 UTC (16:09 LT)
2007	1918 UTC (17:18 LT)	1818 UTC (16:18 LT)	1814 UTC (16:17 LT)

The average SB displacement time between IAG and Campo de Marte Airport was 1 hour. In general, heavy precipitation cells over MASP have been triggered at 1800 UTC. Noteworthily, earlier or later times episodes were weaker, probably due to near surface colder air temperatures and little or no precipitation occurs [1].

The time of the SB front inset allows the nowcasting of heavy rain. The SB front can be monitored by reflectivity MXPOL measurements on clear air mode (Figure 7) together with air and dew point temperatures at the weather stations providing a good tool to predict storms over MASP.

3.2. Rainfall Analysis. Figure 8 shows the spatial distribution of precipitation accumulation within the SPWR surveillance area for all SB episodes. The maximum accumulation was 600 mm downstream from the maximum urbanization in MASP. It agrees with previous studies [12, 24] that indicate downstream sensible heat advection associated with the UHI. Similar rainfall distribution was obtained for all episodes in a given year between 2005 and 2008. A secondary maximum has been observed in Vale do Paraíba (West of MASP) due to valley-mountain differential heating [44].

Figure 9 shows the spatial distribution of the normalized difference vegetation index (NDVI). Lower NDVIs are associated with urban areas [45] and are close to maximum precipitation region over MASP. The current study indicated that 74% of all SB episodes were related to NW winds early afternoon and the maximum rainfall accumulation was downwind of urbanization with lower NDVIs or SE of MASP due to prevailing winds from NW. Baik and Chun [46] and Shepherd et al. [12] found similar results about the advection of HI in other cities. Other rainfall maxima in Figure 8 are related to topography effects.

3.3. Synoptic Patterns and Instability. Hourly mean fields of wind, temperature, and relative humidity at 1000 hPa, 850 hPa, 500 hPa, and 200 hPa pressure levels have been obtained from ARPS runs at 12 km resolution for the 125 SB episodes. Figure 10 shows the 1000-hPa wind field. The results of this research show that ARPS simulation of the time in which the SB has reached IAG's weather station perfectly matches observations (1800 UTC). The wind field direction is from N to NE in early morning and from N to NW in early afternoon and then shifts to SE after 1800 UTC. Figure 11 shows the 1000-hPa mean divergence field with main positive and negative lines of divergence along the coast of São Paulo associated with updrafts (sea breeze) and downdrafts (land breeze), respectively. Figure 14 shows our estimated conceptual model for synoptic conditions for a typical SB episode over MASP. In general, a cold front is moving through over South Brazil, which tends to intensify NW circulation and convergence against the SB front midafternoon.

Vale do Ribeira region is to the SW of MASP about 50-km from the Coastline forming a valley with warmer temperature that induces upward motion and the SB front push earlier than in MASP region. Indeed, we noted that CAPE is generally higher in Vale do Ribeira that accelerates SB front (Figure 12). CAPE values simulated with the ARPS model vary between 1750 J kg^{-1} and 2000 J kg^{-1} over MASP. Results indicate that all SB episodes trigger thunderstorms only under moist unstable environments over MASP. In several SB episodes high CAPE with no CINI inhibit vigorous thunderstorms since CAPE is reduced by generalized convection. Emanuel [47] suggested that under CINI only some convective cells are formed and so updrafts are stronger and induce stronger downdrafts in the nearby environment of the thunderstorms. The mean CINI is −40 J kg^{-1} in MASP so that it hinders convection and CAPE dissipation [47]. The local circulation induced by the UHI yields updrafts over MASP added to the one by the SB front circulation. Figure 15 shows a conceptual model of such circulation with a 2-km deep SB circulation. Since CAPE is only one index of thunderstorm potential, the lifting index, IL [48], was also used. The ARPS mean IL varied between −1.5°C to −2.0°C and −3.5°C to −4.0°C at 1200 UTC and 1600 UTC, respectively. Higher IL has been observed in West and Vale do Ribeira in São Paulo and Mato Grosso do Sul State. They well agree with the warming observed in these regions. The mean CAPE obtained from soundings at Campo de Marte Airport at 1200 UTC was 616 J kg^{-1} against ARPS 559 J kg^{-1} and IL −2.2°C (observed) and −1.5°C (ARPS), respectively. In general, ARPS is in good agreement with observation, though it tends to underestimate IL and properly estimates CAPE.

Synoptic conditions associated with SB episodes show the Bolivian High circulation over Brazil and the South Atlantic subtropical high at low levels with Northerly winds over São Paulo State in the morning. The SB circulation stretches itself throughout the Coastline of Brazil in the afternoon with an average depth of 2-km. In general, a moving cold front in Southern South America is also present. The circulation patterns at 500 hPa and 200 hPa levels are shown in Figure 13. Anticyclonic circulation is over Mato Grosso do Sul and zonal winds are over the São Paulo State (500 hPa) and the circulation is due to Bolivia's high at 200 hPa.

4. Conclusions

The MASP is prone to severe weather with major impacts on society given its steady urban growth in the past decades with microclimate changes induced by anthropic sources that produced the urban heat island effect. It tends to increase precipitation over MASP especially in summer. The warmer urban environment intensifies thunderstorms and

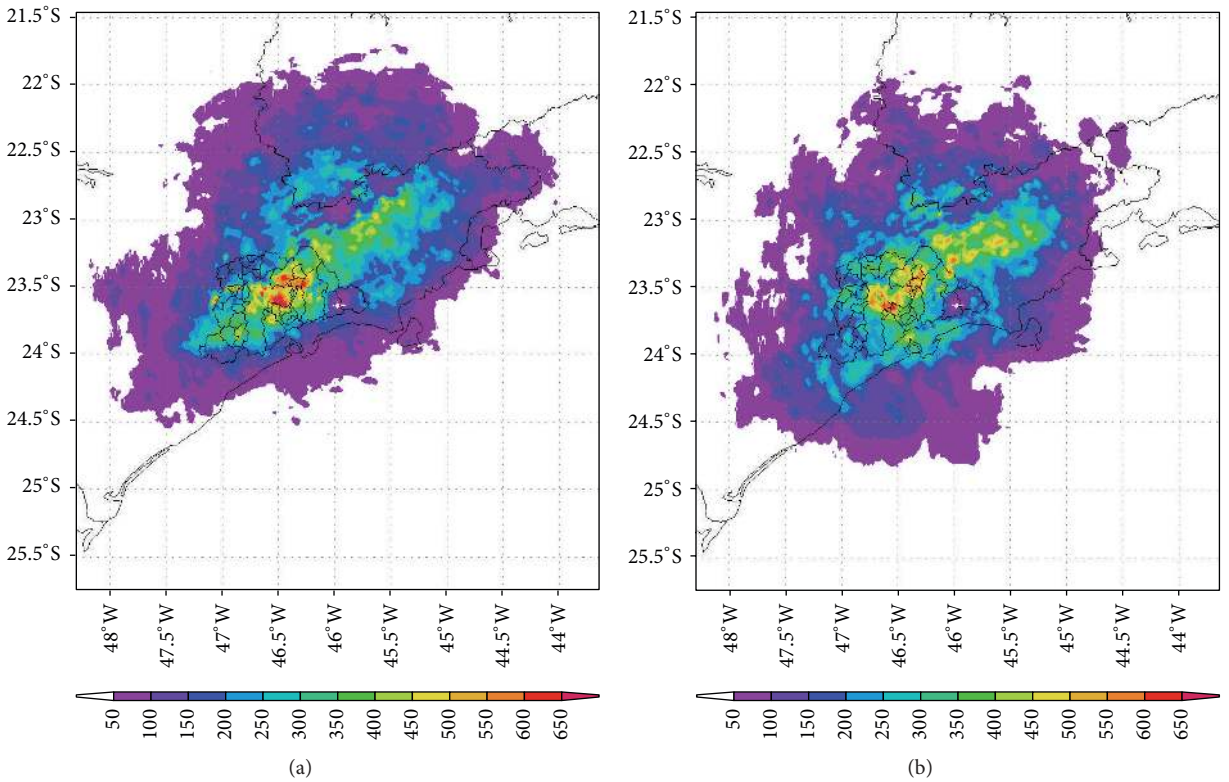

Figure 8: SPWR estimated rainfall accumulation (mm) within its surveillance area in Eastern São Paulo State of all sea breeze events in 2005 (a) and 2007 (b). Contours, geographic boundaries, and political boundaries are indicated.

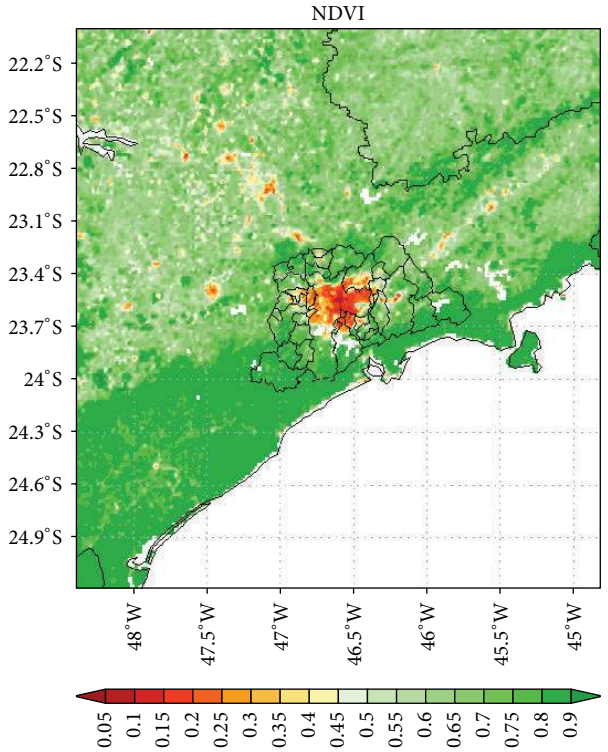

Figure 9: Normalized difference vegetation index (NDVI) within the surveillance area of the SPWR in Eastern São Paulo State. Colors indicate NDVI levels. Contours, geographic boundaries, and political boundaries are indicated.

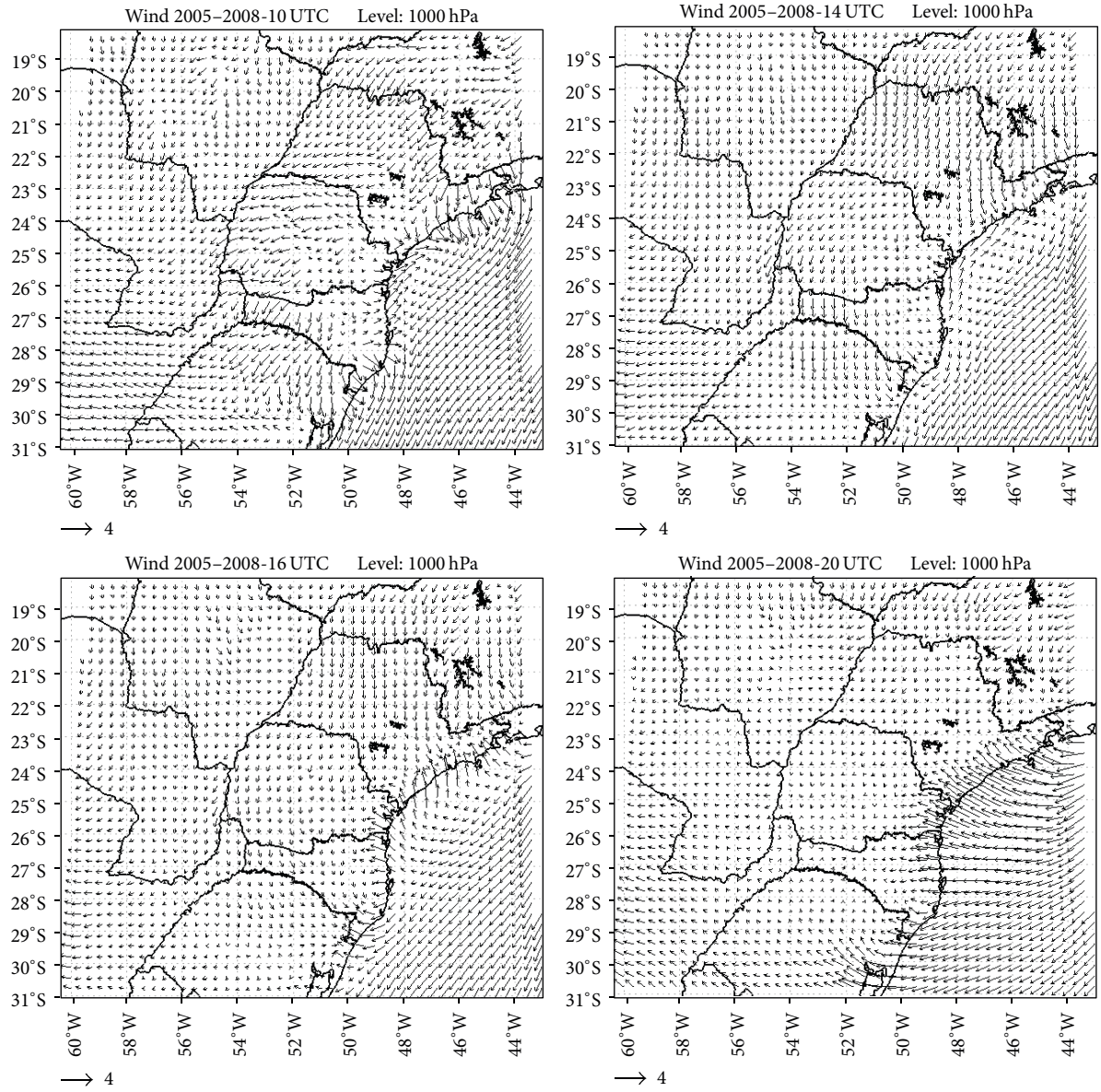

Figure 10: Hourly mean wind field at 1000-hPa between 2005 and 2008 associated with sea breeze and heat island episodes obtained with the ARPS system. Hour, level, contours, and geographic boundaries are indicated.

given impervious urban soil conditions, flash floods, high wind gusts, and other impacts are common. Thunderstorms have been preceded by NW winds in 74% episodes. The SB reaches MASP at about 1800 UTC at IAG weather station and at 1900 UTC at Campo de Marte Airport. At that time, SB circulation had produced very deep thunderstorms over MASP.

The total rainfall field estimated with SPWR has a core of 600 mm over MASP slightly shifted to SE more heavily urbanized. The total rainfall accumulation due to SB episodes is close to half of the annual average at IAG weather station. The Vale do Paraíba region shows a secondary maximum rainfall accumulation as well associated with greater warming and temperature gradients between the mountains and the valley.

The statistics obtained with ARPS simulations well reproduced the diurnal cycle of all days of the year [49]. Maximum CAPE and IL estimated for the afternoon hours were 1750 J kg^{-1} and −3.5°C to −4.0°C, respectively. They are good indicators of conditions favorable to thunderstorm development induced by SB fronts.

Noteworthily, the cold front over southern Brazil plays an important part in intensifying vertical vorticity together with the SB front circulation. In the upper levels under typical summer conditions an anticyclonic circulation is observed and associated with Bolivia's high [50]. The SB circulation interacts with UHI circulation to produce deep thunderstorms. The MXPOL weather radar [40] has been used in conjunction with the ARPS system to nowcasting thunderstorms triggered by these mesoscale features in MASP. Under

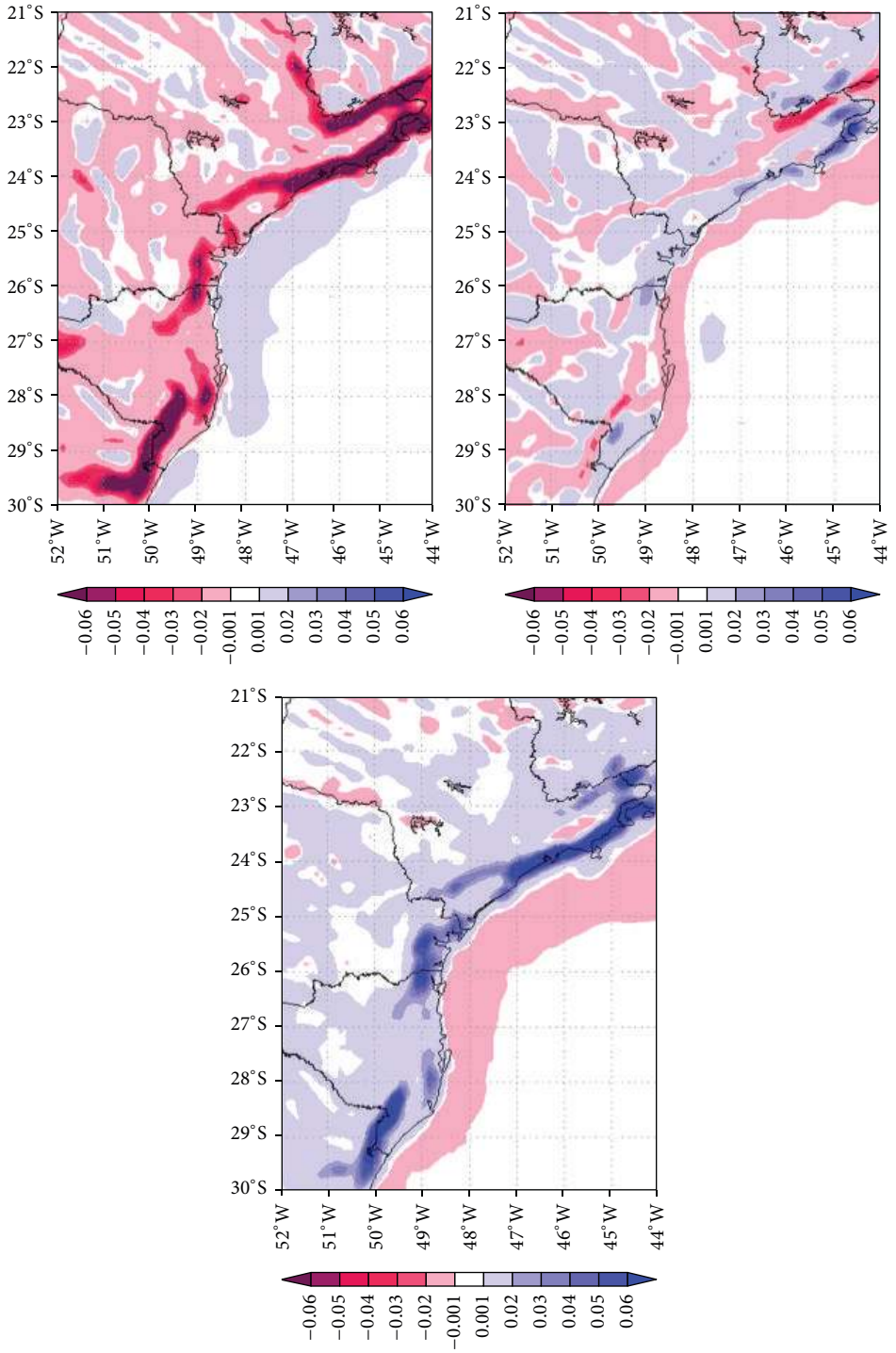

Figure 11: Similar to Figure 10 except for divergence (s^{-1}) at 1000 UTC, 1200 UTC, and 1600 UTC, respectively. Colors indicate divergence (s^{-1}).

certain instability levels and synoptic conditions observed in this research, it is possible to forecast the inset of heavy thunderstorms. These systems are mainly responsible for human and material losses every year. The main findings of this research are useful for nowcasting local and synoptic conditions that will trigger very deep thunderstorms with strong wind gusts, heavy rainfall rates, hail, lightening that in turn will cause damage to urban structures, injuries and casualties, economic losses, and social problems. So, mitigating these anthropic related impacts can be achieved by incorporating local and synoptic features and meteorological variable thresholds such as air and dew point temperatures, wind direction and intensity, and boundaries observed by weather radar and satellite.

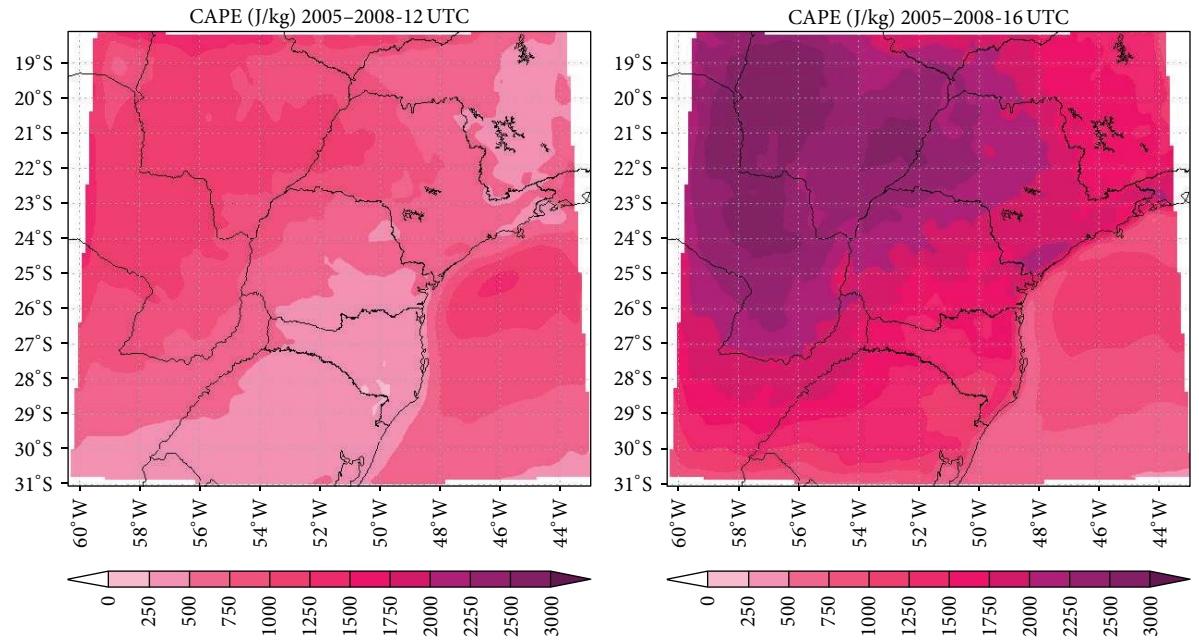

Figure 12: Similar to Figure 10 except for CAPE. Colors indicate CAPE (J kg^{-1}).

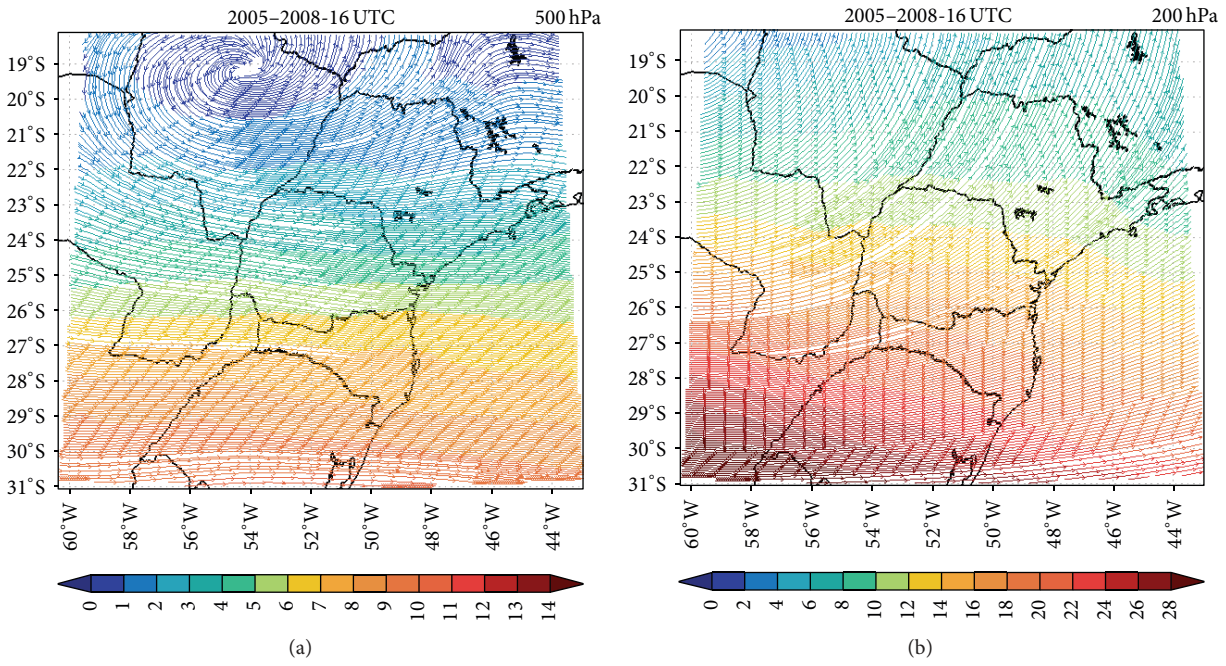

Figure 13: Similar to Figure 10 except for mean wind streamlines at 500 hPa (a) and 200 hPa (b) at 1600 UTC. Colors indicate wind speeds (m s^{-1}).

Conflict of Interests

The authors declare that there is no conflict of interests regarding the publication of this paper.

Acknowledgments

The authors would like to thank IAG, Guarulhos (SBGR), and Congonhas Airports (SBSP) for providing datasets used in this work. The airports data are available in "http://www.redemet.aer.mil.br/index.php?i=produtos&p=plotagem-metar" and IAG data can be obtained from "http://www.estacao.iag.usp.br/sol_dados.php." The CPTEC/INPE provided satellite images that can be obtained from "http://satelite.cptec.inpe.br/." The ARPS system was developed by CAPS and can be downloaded from "http://www.caps.ou.edu/ARPS/arpsdown.html." The data from São Paulo weather radar can be obtained by sending an email to radar@saisp.br. The authors

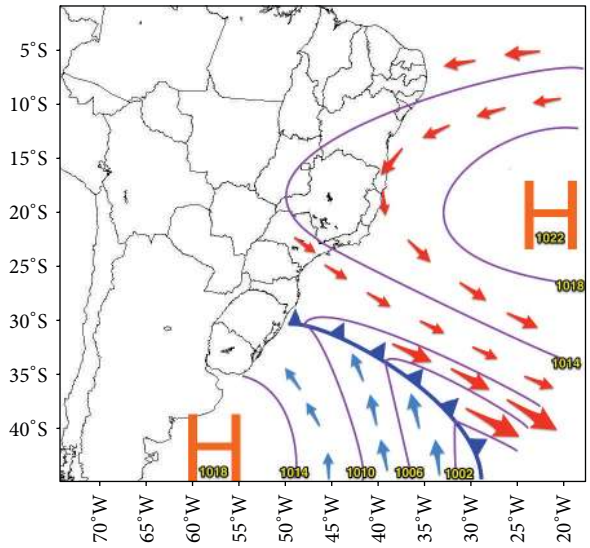

Figure 14: Schematics of a typical synoptic condition associated with deep convection development over MASP caused by intense sea breeze and heat island circulation. Isobars (hPa) and winds and frontal boundaries are indicated.

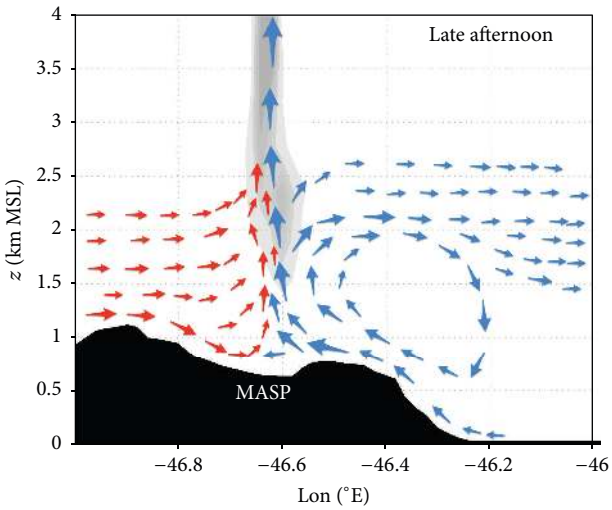

Figure 15: Schematics of a late afternoon cross-section of local winds and cloudiness observed for a typical deep convection development over MASP caused by sea breeze and local heat island.

can provide data from MXPOL weather radar that was generated according to description in Pereira Filho [40]. The sounding data are available in "http://weather.uwyo.edu/upperair/sounding.html." This research is supported by CAPES and CNPq.

References

[1] A. J. Pereira Filho, M. T. L. Barros, R. Hallak, and A. W. Gandu, "Enchentes na região metropolitana de São Paulo: aspectos de mesoescala e avaliação de impactos," in *Proceedings of the 13th Congresso Brasileiro de Meteorologia*, pp. 28–93, Fortaleza, Brazil, September 2004, (Portuguese).

[2] A. J. Pereira Filho, R. Haas, and T. Ambrizzi, "Caracterização dos eventos de cnchente na Bacia do Alto Tietê por meio do radar meteorológico e da modelagem numérica de mesoescala," in *XII Congresso Brasileiro de Meteorologia*, Foz do Iguaçu, Brazil, August 2002 (Portuguese).

[3] A. J. Pereira Filho, "Chuvas de verão e as enchentes na grande São Paulo: el niño, brisa marítima e ilha de calor," in *I Seminário Brasileiro de Hidrometeorologia and XI Congresso Brasileiro de Meteorologia*, Rio de Janeiro, Brazil, 2000 (Portuguese).

[4] A. P. Oliveira and P. L. S. Dias, "Aspectos observacionais da brisa marítima em São Paulo," in *II Congresso Brasileiro de Meteorologia*, vol. 2, pp. 129–161, Pelotas, Brazil, October 1982 (Portuguese).

[5] A. J. Pereira Filho, O. Massambani, R. Hallak, and H. Karam, "A hidrometeorological forecast system for the Metropolitana Area of São Paulo," in *Proceedings of the World Weather Research Programme's Symposium on Nowcasting and Very Short Range Forecasting (WSN '05)*, Toulouse, France, 2005.

[6] W. T. Thompson, T. Holt, and J. Pullen, "Investigation of a sea breeze front in an urban environment," *Quarterly Journal of the Royal Meteorological Society*, vol. 133, no. 624, pp. 579–594, 2007.

[7] A. Dandou, M. Tombrou, and N. Soulakellis, "The influence of the City of Athens on the evolution of the sea-breeze front," *Boundary-Layer Meteorology*, vol. 131, no. 1, pp. 35–51, 2009.

[8] F. J. Robinson, M. D. Patterson, and S. C. Sherwood, "A numerical modeling study of the propagation of idealized sea-breeze density currents," *Journal of the Atmospheric Sciences*, vol. 70, no. 2, pp. 653–668, 2013.

[9] A. N. F. Porson, D. G. Steyn, and G. Schayes, "Formulation of an index for sea breezes in opposing winds," *Journal of Applied Meteorology and Climatology*, vol. 46, no. 8, pp. 1257–1263, 2007.

[10] B. W. Atkinson, *Meso-Scale Atmospheric Circulation*, vol. 495, Academic Press, London, UK, 1981.

[11] G. Ganbat, J. M. Seo, J.-Y. Han, and J.-J. Baik, "A theoretical study of the interactions of urban breeze circulation with mountain slope winds," *Theoretical and Applied Climatology*, vol. 121, no. 3, pp. 545–555, 2015.

[12] J. M. Shepherd, H. Pierce, and A. J. Negri, "Rainfall modification by major urban areas: Observations from spaceborne rain radar on the TRMM satellite," *Journal of Applied Meteorology*, vol. 41, no. 7, pp. 689–701, 2002.

[13] H. Kusaka, K. Nawata, A. Suzuki-Parker, Y. Takane, and N. Furuhashi, "Mechanism of precipitation increase with urbanization in Tokyo as revealed by ensemble climate simulations," *Journal of Applied Meteorology and Climatology*, vol. 53, no. 4, pp. 824–839, 2014.

[14] E. Marques Filho, H. Karam, A. Miranda, and A. França Junior, "Rio de Janeiro's tropical urban climate," *News Letter of the Internation Association of Urban Climate*, vol. 32, pp. 5–9, 2009.

[15] E. D. Freitas and P. L. S. Dias, "Alguns efeitos de áreas urbanas na geração de uma ilha de calor," *Revista Brasileira de Meteorologia*, vol. 20, no. 3, pp. 355–366, 2005.

[16] T. R. Oke, *Boundary Layer Climates*, Routledge, London, UK, 1978.

[17] T. Meir, P. M. Orton, J. Pullen, T. Holt, and W. T. Thompson, "Forecasting the New York City urban heat island and sea breeze during extreme heat events," *Weather and Forecasting*, vol. 28, no. 6, pp. 1460–1477, 2013.

[18] M. J. Ferreira, *Estudo do balanço de energia na superfície aplicado a cidade de São Paulo [Ph.D. thesis]*, Department of Atmospheric Science, University of São Paulo, São Paulo, Brazil, 2010.

[19] I. Eliasson, "Urban nocturnal temperatures, street geometry and land use," *Atmospheric Environment*, vol. 30, no. 3, pp. 379–392, 1996.

[20] J. L. Flores, H. A. Karam, E. P. M. Filho, and A. J. P. Filho, "Estimation of atmospheric turbidity and surface radiative parameters using broadband clear sky solar irradiance models in Rio de Janeiro-Brasil," *Theoretical and Applied Climatology*, 2015.

[21] H. E. Landsberg, *The Urban Climate*, Academic Press, New York, NY, USA, 1981.

[22] J. D. Fast and M. D. McCorcle, "A two-dimensional numerical sensitivity study of the great plains low-level jet," *Monthly Weather Review*, vol. 118, no. 1, pp. 151–163, 1990.

[23] G.-X. He, C. W. F. Yu, C. Lu, and Q.-H. Deng, "The influence of synoptic pattern and atmospheric boundary layer on PM10 and urban heat island," *Indoor and Built Environment*, vol. 22, no. 5, pp. 796–807, 2013.

[24] J.-Y. Han, J.-J. Baik, and H. Lee, "Urban impacts on precipitation," *Asia-Pacific Journal of Atmospheric Sciences*, vol. 50, no. 1, pp. 17–30, 2014.

[25] E. D. Freitas, C. M. Rozoff, W. R. Cotton, and P. L. Silva Dias, "Interactions of an urban heat island and sea-breeze circulations during winter over the metropolitan area of São Paulo, Brazil," *Boundary-Layer Meteorology*, vol. 122, no. 1, pp. 43–65, 2007.

[26] W. R. G. Farias, O. Pinto Jr., K. P. Naccarato, and I. R. C. A. Pinto, "Anomalous lightning activity over the Metropolitan Region of São Paulo due to urban effects," *Atmospheric Research*, vol. 91, no. 2–4, pp. 485–490, 2009.

[27] H. B. Blueinstein, *Synoptic-Dynamic Meteorology in Midlatitudes. Volume II: Observations and Theory of Weather Systems*, Oxford University Press, New York, NY, USA, 1993.

[28] R. A. Anthes, "Numerical prediction of severe storms—certainty, possibility or dream?" *Bulletin of the American Meteorological Society*, vol. 57, pp. 423–430, 1976.

[29] W. R. Cotton and R. A. Anthes, *Storm and Cloud Dynamics*, Academic Press, EUA, San Diego, Calif, USA, 1989.

[30] R. H. Johnson and B. E. Mapes, "Mesoescale processes and severe convective weather," in *Severe Convective Storms*, C. A. D. Doswell III, Ed., vol. 28 of *Meteorological Monographs*, American Meteorological Society, 2001.

[31] E. C. Vicente, C. A. Sangiolo, and A. J. Pereira Filho, "Características das precipitações convectivas intensas na area do radar meteorológico de São Paulo," in *XII Congresso Brasileiro de Meteorologia*, Poços de Caldas, Brazil, August 2002.

[32] P. J. Roebber, D. M. Schultz, B. A. Colle, and D. J. Stensrud, "Toward improved prediction: high-resolution and ensemble modeling systems in operations," *Weather and Forecasting*, vol. 19, no. 5, pp. 936–949, 2004.

[33] M. Xue, K. K. Droegemeier, and V. Wong, "The Advanced Regional Prediction System (ARPS)—a multi-scale nonhydrostatic atmospheric simulation and prediction model. Part I: model dynamics and verification," *Meteorology and Atmospheric Physics*, vol. 75, no. 3-4, pp. 161–193, 2000.

[34] M. Xue, K. K. Droegemeier, V. Wong et al., "The Advanced Regional Prediction System (ARPS)—a multi-scale nonhydrostatic atmospheric simulation and prediction tool. Part II: model physics and applications," *Meteorology and Atmospheric Physics*, vol. 76, no. 3-4, pp. 143–165, 2001.

[35] M. Xue, D. Wang, J. Gao, K. Brewster, and K. K. Droegemeier, "The Advanced Regional Prediction System (ARPS), storm-scale numerical weather prediction and data assimilation," *Meteorology and Atmospheric Physics*, vol. 82, pp. 139–170, 2003.

[36] M. Xue and W. J. Martin, "A high-resolution modeling study of the 24 May 2002 dryline case during IHOP. Part II: horizontal convective rolls and convective initiation," *Monthly Weather Review*, vol. 134, no. 1, pp. 172–191, 2006.

[37] R. Hallak, A. J. Pereira Filho, A. W. Gandu, and M. T. Barros, "Simulação numérica de precipitação intense na Região Metropolitana de São Paulo com o modelo de mesoescala ARPS," in *Proceedings of the 13th Congresso Brasileiro de Meteorologia*, Fortaleza, Brazil, September 2004.

[38] R. Hallak, *Simulações numéricas de tempestades severas na RMSP [Ph.D. thesis]*, Department of Atmospheric Science, University of São Paulo, São Paulo, Brazil, 2007.

[39] F. W. Menezes, *Tempestades severas: um modelo para latitudes subtropicais [Ph.D. thesis]*, Department of Atmospheric Science, University of São Paulo, São Paulo, Brazil, 1998.

[40] A. J. Pereira Filho, "A mobile X-POL weather radar for hydrometeorological applications in the metropolitan area of São Paulo, Brazil," *Geoscientific Instrumentation, Methods and Data Systems*, vol. 1, no. 2, pp. 169–183, 2012.

[41] J. S. Marshall and W. M. K. Palmer, "The distribution of raindrops with size," *Journal of Atmospheric Sciences*, vol. 5, no. 4, pp. 165–166, 1948.

[42] M. Xue, K. K. Droegemeier, W. Wong, A. Shapiro, and K. Brewster, *Advanced Regional Prediction System Users Guide*, University of Oklahoma, Norman, Okla, USA, 1995.

[43] C. A. M. Rodriguez, R. P. da Rocha, and R. J. Bombardi, "On the development of summer thunderstorms in the city of São Paulo: mean meteorological characteristics and pollution effect," *Atmospheric Research*, vol. 96, no. 2-3, pp. 477–488, 2010.

[44] H. Tong, A. Walton, J. Sang, and J. C. L. Chan, "Numerical simulation of the urban boundary layer over the complex terrain of Hong Kong," *Atmospheric Environment*, vol. 39, no. 19, pp. 3549–3563, 2005.

[45] T. N. Carlson and D. A. Ripley, "On the relation between NDVI, fractional vegetation cover, and leaf area index," *Remote Sensing of Environment*, vol. 62, no. 3, pp. 241–252, 1997.

[46] J.-J. Baik and H.-Y. Chun, "A dynamical model for urban heat islands," *Boundary-Layer Meteorology*, vol. 83, no. 3, pp. 463–477, 1997.

[47] K. Emanuel, *Atmospheric Convection*, Oxford University Press, 1994.

[48] J. G. Galway, "The lifted index as a predictor of latent instability," *Bulletin of the American Meteorological Society*, vol. 37, pp. 528–529, 1956.

[49] A. P. Oliveira, R. D. Bornstein, and J. Soares, "Annual and diurnal wind patterns in the city of São Paulo," *Water, Air, and Soil Pollution: Focus (Prelo)*, vol. 3, no. 5, pp. 3–15, 2003.

[50] P. L. Silva Dias, W. H. Schubert, and M. DeMaria, "Large-scale response of the tropical atmosphere to transient convection," *Journal of the Atmospheric Sciences*, vol. 40, no. 11, pp. 2689–2707, 1983.